

Water-Dispersible Rhodamine B Hydrazide Loaded TiO₂ Nanoparticles for “Turn On” Fluorimetric Detection and Imaging of Orthosilicic Acid Accumulation *In-Vitro* in Nephrotoxic Kidney Cells

Starlaine C. Mascarenhas^{1,†}, Ram U. Gawas^{2,†}, Barun Kumar Ghosh², Mainak Banerjee²,
Anasuya Ganguly^{1,*}, Amrita Chatterjee^{2,*}, and Narendra Nath Ghosh^{2,*}

¹Department of Biological Sciences, and ²Department of Chemistry, Birla Institute of Technology and Science,
Pilani K K Birla Goa Campus, Zuarinagar, Goa 403726, India

Silica (SiO₂) is the inevitable form of silicon owing to its high affinity for oxygen, existing as a geogenic element perpetrating multifarious health problems when bioavailable via anthropogenic activities. The hydrated form of silica viz. orthosilicic acid (H₄SiO₄) excessively displays grave toxicity, attributed to prolonged exposure and incessant H⁺ ions generating capacity inflicting pulmonary toxicity and renal toxicity silica. The diverse deleterious potency of silica highlights the desirability of selective and sensitive detection of toxic species (mainly orthosilicic acid) bioaccumulation in affected living human cells. In this paper we have reported, the design of water-dispersible turn-on fluorimetric sensing material for the detection of orthosilicic acid in the aqueous phase and in live cells. The sensing material was prepared by adsorbing a suitable rhodamine derivative (i.e., Rhodamine B hydrazide (Rh1)) on water dispersible TiO₂ nanoparticles. The function of the sensing system, which is composed of Rh1 and TiO₂ (Rh1@TiO₂), is accredited to H⁺ ion (from orthosilicic acid) induced spirolactam ring-opening of the rhodamine derivative generating orange fluorescence and bright pink colouration. The sensing system was efficiently utilized for fluorimetric detection and imaging of orthosilicic acid accumulation *in-vitro* in human kidney cells (HK cells). To the best of our knowledge, this is the first time this sensing system (Rh1@TiO₂) is reported for detection of toxic silica species accumulation *in-vitro* in human kidney cells. The advantages, such as good water dispersibility, the absence of organic solvents during fluorimetric studies, quick turn-on type signal transduction, low-level imaging, which are offered by the synthesized sensing material (Rh1@TiO₂), make it a potential candidate to fabricate medical tool for early identification of silica-induced nephrotoxicity, which can help to reduce the burden and risk of chronic kidney disease development.

Keywords: TiO₂ Nanoparticles, Rhodamine Dependent Fluorimetry, Nanomaterial-Based Sensor, Nephrotoxic Silica, Bio-Imaging of Live Cells, Human Kidney (HK) Cells.

1. INTRODUCTION

Silicon is the second most abundant constituent contributing to 28% of earth's crust. Silicon being highly reactive converts from its elemental form and combines either with oxygen forming free silica (SiO₂) or with

other elements and oxygen forming silicates, like asbestos, quartz, feldspar etc.¹ Silica is abundantly present in rocks, sand and soil. However, it is not readily bioavailable as it remains combined with oxygen and hence is generally categorised as a trace geogenic element.² The threat arises when silica emanates in air and water during the course of various anthropogenic activities, like granite mining, sand mining, etc., manifesting serious health problems

*Authors to whom correspondence should be addressed.

[†]These two authors contributed equally to this work.

including silicosis,^{3,4} bronchitis,⁵ systemic autoimmune diseases like rheumatoid arthritis (RA),⁶ systemic lupus erythematosus (SLE)⁷ and systemic sclerosis (SSc),⁸ lung cancer.⁹ Due to grave toxicity exhibited by silica, OSHA has set harsh regulations limits to 50 $\mu\text{g}/\text{m}^3$ in air.¹⁰

In recent times, limited epidemiological reports have highlighted the potential of silica to exhibit nephrotoxicity as well, resulting mainly in chronic kidney disease development.^{11–13} The hydrated form of silica (orthosilicic acid, H₄SiO₄) at a concentration range of 100–120 mg/L induces severe nephrotoxicity on prolonged exposure, accredited to its bioaccumulative propensity.^{14,15} However, in spite of silica's diverse toxicological potential, studies analysing cellular penetration and accumulation of silica in targeted mammalian cells (specifically human cells) on prolonged exposure, an essential prerequisite for toxicity, are unavailable till date. Few reports utilised labour intensive and expensive instrumentation like SEM coupled with X-ray analysis,¹⁶ X-ray fluorescence spectrometer (P-XRF) for silica deposit visualisation in grasses¹⁷ and diatoms.¹⁸ However, these techniques suffer from major limitations of longer data acquisition time, necessity of sophisticated and expensive instrumentation, requirement of trained personnel, tedious sample preparation (such as solubilisation or *in-situ* charring of cells to estimate the silica content), thereby negating the possibility of its application in live human cell imaging of silica species. Owing to its trace amounts, influences of coexisting substances in real samples, rising and severe deleterious effects induced by bioaccumulated silica species and limitations of the analytical techniques, the development of sensitive, rapid on-site detection of toxic silica species (especially orthosilicic acid) and imaging of silica contaminated live mammalian cells are necessary.

Fluorimetric techniques involving small organic molecules as chemo-reactants or chemo-dosimeters are well-validated methods for the detection of toxic analytes or even imaging of biological species due to high selectivity and sensitivity, instant signal transduction, low-cost instrumentation etc.^{19,20} In this context, rhodamine with high quantum yield is a vastly used fluorophore for molecular sensing of various analytes,^{21,22} which often sense the analytes by the opening of its non-fluorescent spiro-lactam ring to a highly fluorescent and coloured form.²³ Some rhodamine derivatives have successfully utilized this principle in developing fluorimetric and colourimetric probes for the determination of pH of a solution;^{24–26} the present method is based on the same principle. Relevant to this, a couple of rhodamine derivatives have also been used as simple dyes for the detection of silica deposition in diatoms based on the formation of orthosilicic acid via dissolution of silica in the aqueous intra-cellular environment.^{27,28} However, use of some amount of organic solvents is inevitable to dissolve these

organic dyes in the working solution. This is a serious concern for biotechnological applications as organic solvents can exaggerate severe toxicity to biological systems restricting their application in live cells or any other living species. One of the possible ways to overcome this difficulty is the use of water-dispersible nanomaterials on which a chemodosimeter can be grafted by physical or chemical modifications.

Nanomaterials, many of which possess excellent water dispersibility, enormous surface area/volume ratio, large adsorption capacity, great mechanical strength and surface reactivity, intrinsic optical/electrochemical/magnetic/spectroscopic properties, have proved their efficacy in recent years as suitable candidates for the development of material based sensors by selective interactions of their surface (pre-functionalized with the signal transduction unit) with the analytes.^{29,30} Often nanomaterial-based chemosensors outshine traditional detection techniques with decreased sampling time, quicker analytical response, high sensitivity and low cytotoxicity.^{31,32} Some of the nanomaterials comprehensively used for biological and environmental assessment of lethal analytes include metal nanoparticles (e.g., Au, and Ag nanoparticles), carbon materials (carbon nanotubes, and graphene), magnetic nanoparticles (e.g., Fe, Ni, Co), quantum dots (such as ZnS, CdTe, and CdSe) and metal-oxide nanomaterials (viz. TiO₂, CuO, ZnO, etc.).^{33,34} Of our interest, TiO₂ nanoparticles are good candidates to be used as matrix for sensing purpose owing to its unique properties including enhanced adsorptive surface area,³⁵ resistance to photo and chemical erosion,³⁶ chemical and biological inertness,³⁷ low-cost synthesis, monodispersity,³⁸ and nontoxicity.³⁹ Moreover, excellent biocompatibility⁴⁰ and easy cellular uptake on dispersion in aqueous media⁴¹ further extends its potential application for live-cell imaging of intracellular toxic silica species deposits.

Interactions of Nanomaterials with the biological systems have been investigated by several researchers.^{42–43} As a part of our continuous efforts on the development of molecular probes for biological and environmentally noxious analytes^{44–51} we report, herein, a water-dispersible “turn-on” fluorimetric sensing material, which is comprised of rhodamine-B based chemodosimeter (rhodamine B hydrazide (Rh1)) and TiO₂ nanoparticles (Rh1@TiO₂), for the detection and imaging of toxic silica species (viz. orthosilicic acid) bioaccumulation in live cells. We chose rhodamine B hydrazide (Rh1) as the chemodosimeter unit, which was first reported by Dujols et al.⁵² as a sensor for Cu(II) ions in water and later used by others^{53–62} for various sensing and imaging studies. It was presumed that the acidic environment inside the cell would induce spiro-lactam ring-opening and transduce fluorescence.^{23,57} To demonstrate our concept silica affected nephrotoxic kidney cells were chosen.

2. EXPERIMENTAL DETAILS

2.1. Chemicals

Rhodamine B HCl and Hydrazine hydrate were purchased from Sigma Aldrich (India) and used as received. TiCl₃ was purchased from Spectrochem Pvt. Ltd. Mumbai (India). Ethylene diamine tetra acetic acid (EDTA) was purchased from Merck, India. All solvents and other chemicals were of AR grade and were procured from different commercial suppliers and used without further purification. Millipore water (18 MΩ) was used for all spectroscopic studies.

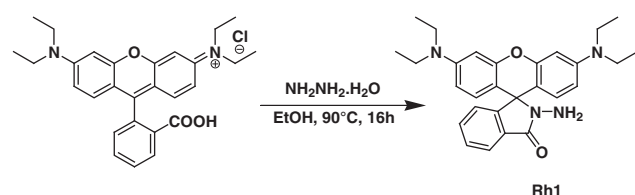
2.2. Instruments and Measurements

NMR spectra were recorded on Bruker Avance (400 MHz) NMR spectrometer. Mass spectra were obtained from Agilent technologies 6460 triple quad LC-MS (ESI). Fluorescence spectra were measured on a JASCO FP-6300 spectrofluorometer, the slit width was 2.5 nm for both excitation and emission. Absorption spectra were recorded on a JASCO V570 UV/Vis/NIR spectrophotometer. Infrared spectra were taken on IR Affinity-1 FTIR spectrophotometer, Shimadzu. Elemental analysis was carried out on Vario elemental CHNS analyzer. Thermogravimetric analysis (TGA) data were recorded using a DTG-60, Shimadzu. Field Emission Scanning Electron Microscopy (FESEM) images of the TiO₂ nanoparticles were obtained on FESEM Quanta 250 FEG (FEI) with 10 kV and resolution 2 nm. The powder X-ray diffraction (XRD) patterns were obtained from powder X-ray diffractometer (Mini Flex II, Rigaku, Japan).

2.3. Synthesis of Materials

2.3.1. Preparation of Rhodamine Hydrazide (Rh1)

The chemodosimeter, Rh1 was prepared according to a reported method^{53,63} (Scheme 1). In a 100 ml round bottom flask, rhodamine B (1.0 g, 2.08 mM) was dissolved in 15 ml absolute alcohol, to which excess of Hydrazine hydrate (98%, 2.08 g, 4.16 mM) was added under stirring at room temperature. The reaction mixture was then refluxed for 16 h at 110 °C. After completion of the reaction, 10 ml water was added and the residue was filtered, washed with water (3 × 10 mL), and then air-dried. The crude product was recrystallized from the ethanol-water mixture to obtain the sufficiently pure product, Rh1 (650 mg, 67.5% yield).



Scheme 1. Synthesis of rhodamine B hydrazide (Rh1).

2.3.2. Preparation of TiO₂ Nanoparticle

TiO₂ nanoparticles were prepared using an EDTA precursor based method, which was developed by Ghosh and coworkers.⁶⁴ In a 250 mL glass beaker, 21.1 mL of TiCl₃ (192.6 mM) was taken, and then an aqueous solution of HNO₃ was added to it dropwise to oxidized Ti³⁺ to Ti⁴⁺. Separately, in a beaker aqueous solution of EDTA (10% w/v) was prepared by dissolving EDTA in hot water with dropwise addition of dilute NH₄OH solution. After complete dissolution of EDTA, the solution was boiled to remove excess NH₃. This EDTA solution was then added to a solution containing Ti⁴⁺ ions (keeping Ti⁴⁺:EDTA molar ratio 1:1) with constant stirring. The reaction mixture was evaporated to dryness over a hot plate at 125 °C to obtain the precursor powder for TiO₂. Finally, the precursor was calcined at 550 °C for 3 h to obtain TiO₂ nanoparticles with an average diameter of ~35 nm.

2.3.3. Preparation of the Sensing Material, Rh1@TiO₂

For the grafting of Rh1 onto the TiO₂ nanoparticles, 100 mg of sonicated TiO₂ nanoparticles was added to Rh1 (10 mg, 0.022 mM) in dry acetonitrile solution (100 mL) and magnetically stirred in the dark for 60 min to ensure it reaches adsorption–desorption equilibrium.⁶⁵ The Rh1 adsorbed TiO₂ nanoparticles (Rh1@TiO₂) were collected by centrifugation at 2500 rpm for 5 min followed by washing the residue with acetonitrile (2 × 25 mL) and dried in a vacuum desiccator (in the dark) for 4 h to obtain a white solid (110 mg, 100% yield) as the final sensing material.

2.3.4. The General Procedure of Sample Preparation for Fluorescence Measurement

10 mg of the probe Rh1@TiO₂ was dispersed in 10 mL of deionized water (MilliQ, 18 MΩ) to get a 1 g/L of the stock solution as and when required and diluted further as per requirement. 1 g/L (10 mM) stock solution of orthosilicic acid was prepared in deionized water and diluted further for the preparation of working solutions. To analyse the effect of different metal ions stock solutions (10 mM, 5 mL) were prepared by dissolving their respective nitrates/chlorides in deionized water. All analyte solutions were subjected to 0.22 μm syringe filtration to avoid any interference by particulate matter in fluorescence measurement. After analyte addition, each solution was incubated for 10 min before recording their respective fluorescence spectrum at an excitation wavelength of 525 nm and the emission was recorded from 526 to 650 nm. All the experiments were executed at room temperature. For the equivalence study, orthosilicic acid doses were altered from 0–100 μL of 10 mM (or 0.0–33.3 mg/L) for fluorescence measurement.

2.3.5. General Procedure for Fluorescence Study

The fluorescence study was carried out by addition of 30 μL of the sensing material, Rh1@TiO₂ (1 g/L stock

solution) in deionized water (3 mL) in a cuvette. To this solution, increasing amount of orthosilicic acid (1 g/L stock solution) were added and fluorescence response was measured after every 10 min, respectively. For equivalent study concentrations of orthosilicic acid were changed from 0–33.3 mg/L (i.e., 0–105 μ L from stock solution). For each reaction mixture fluorescence response was recorded. The same procedure was followed for comparative study with other metal ions.

2.3.6. Procedure for pH Dependency Study

For the preparation of acidic pH solutions, sodium acetate in the acetic acid buffer and for basic pH solutions phosphate buffer was used. The pH dependency study was carried out by addition of 30 μ L of Rh1@TiO₂ sensing material (from 1 g/L stock) in 3 mL of each individual pH buffer (ranging from 3–10) in a cuvette and the fluorescence response was recorded. This was followed by addition of 30 μ L of orthosilicic acid (1 g/L) to each individual pH buffer solution containing the Rh1@TiO₂ sensing material and the fluorescence intensity was recorded after 10 min incubation.

2.3.7. Cytotoxicity Study

Cytotoxicity of Rh1@TiO₂ was tested using the colourimetric MTT assay.⁶⁴ HK cells (Human Kidney cells) were cultured in Dulbecco's Modified Eagle's Medium (DMEM) supplemented with 10% (v/v) fetal bovine serum at 37 °C and humidified 5% CO₂. 5 × 10⁴ cells were plated per well in a 24-well plate. Rh1@TiO₂ (1 g/L) was dissolved in aqueous PBS (pH 7) to make a stock solution. Following 24 h incubation, the cells were dosed with increasing concentrations of the sensing material, Rh1@TiO₂ (1, 10, 50, 100, and 200 mg/L) formulated by serial dilution in DMEM. Unexposed controls were maintained. After an additional 24 h incubation, 50 μ L of MTT (5 mg/mL in PBS) was added per well and incubated for 4 h. Following which the media was aspirated from the wells, 0.5 mL of DMSO was added. Absorbance was recorded at 570 nm and cell viability was expressed as a percentage of relative absorbance of the sample versus unexposed control cells for every probe concentration. Each set of experiments were triplicated and the average results are presented.

2.3.8. Fluorescence Imaging of Toxic Silica Species in Living Cells

For fluorescence imaging of silica (viz. orthosilicic acid) accumulation in living cells, HK cells were chosen. HK cells were plated in a 6-well plate in Dulbecco's modified Eagle's medium (DMEM) supplemented with 10% fetal bovine serum for 24 h. The cells were then incubated with increasing doses of silica (0.1, 1, 10 and 100 mg/L) for three different time points (1 h, 24 h, and 8 days), followed by treatment with the sensing material (100 μ L of

1 g/L of stock solution) was added to 2 mL of culture medium) at 37 °C and 5% CO₂ for 30 min. Fluorescence images were captured by a fluorescence microscope (Olympus IX51) under a TRITC filter and reported. Each experimental study was triplicated to ensure enhanced data reproducibility.

3. RESULTS AND DISCUSSION

3.1. Characterizations of the Synthesized Rh1, TiO₂ Nanoparticles, and Rh1@TiO₂

The synthesized materials were characterized by using several instrumental techniques, such as ¹H NMR, ¹³C NMR, ESI-MS, IR, CHN, XRD, TGA, and FESEM. Rh1 was characterized by ¹H NMR, ¹³C NMR, ESI-MS, IR and CHN. The ¹H and ¹³C NMR spectra of the Rh1 are shown in Figures 1 and 2, respectively and the obtained data are in well-agreement with the reported values of Rh1.^{50,61} Mass spectroscopy analysis ($m/z = 457$ [M + H]⁺) and CHN analysis (Calculated C, H and N amount for C₂₈H₃₂N₄O₂: C: 73.66; H: 7.06; N: 12.27 and data obtained from CHN analysis: C: 73.59; H: 6.99; N: 12.19) of the product also confirmed the formation of Rh1 (molecular formula C₂₈H₃₂N₄O₂).

The crystalline phase and crystallite size of the synthesized TiO₂ were determined by using XRD. XRD pattern of the synthesised TiO₂ nanoparticles (Fig. 3) showed the presence of peaks at $2\theta = 25.3^\circ$, 37.8° , 48.1° , 53.9° , and 55.06° , which are corresponding to the (101), (004), (200), (105) and (211) planes of anatase phase [JCPDS Card no. 21-1272], and confirmed the formation of the pure anatase phase of TiO₂. The crystallite size of the synthesized TiO₂ nanoparticles (calculated by using Scherrer equation) was found to be ~38 nm.

The sensing material, Rh1@TiO₂ was prepared by grafting TiO₂ nanoparticles with Rh1. The thermogravimetric analysis (TGA) was utilized to determine the amount of Rh1 in Rh1@TiO₂ (Fig. 4). TGA thermograms showed that pure Rh1 was fully decomposed within the temperature range of 600 °C, whereas TiO₂ nanoparticles were quite stable in this temperature range. In case of Rh1@TiO₂, 8% weight loss was observed when the sample was heated up to 600 °C, which indicated that Rh1@TiO₂ is composed of 8 wt% Rh1 and 92 wt% of TiO₂. This is in well-agreement with the ratio of the probe, Rh1 and TiO₂ used during the synthesis (1:10), and it can be concluded that almost 90% of the Rh1 successfully adhered onto the surface of TiO₂ nanoparticles.

In the IR spectra of Rh1@TiO₂ (Fig. 5) the presence of the signature peaks of Rh1 (IR bands at 3340, 3082, 2969, 1774, 1618, 1519, 1272, 1115 cm⁻¹) also indicated the physisorption of Rh1 on TiO₂.

SEM micrographs revealed that the diameter of TiO₂ nanoparticles was in the range of 25–6 nm, with an average of ~35 nm (Fig. 6(A)). SEM images of Rh1@TiO₂ also

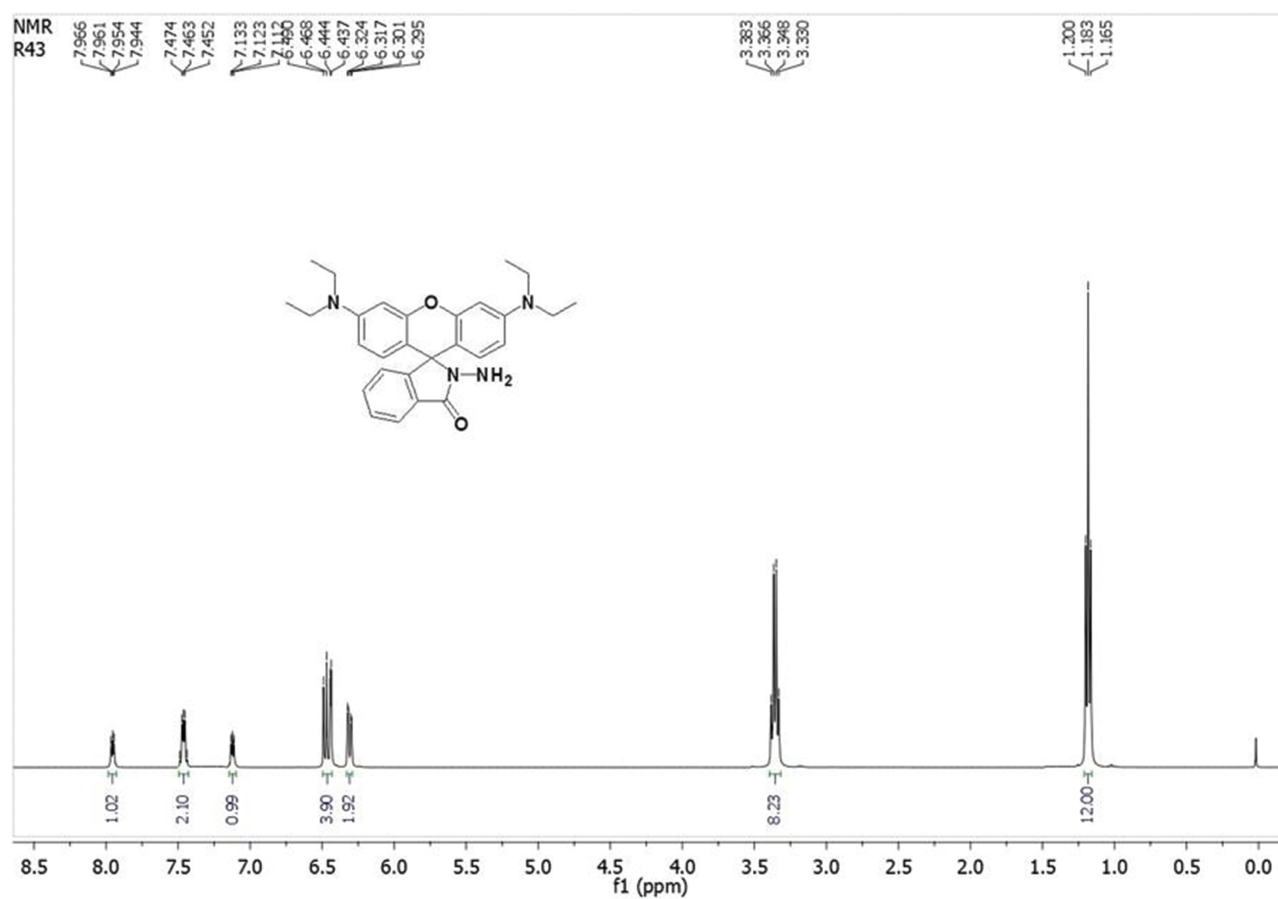


Figure 1. ¹H NMR spectra of Rh1 (¹H NMR (400 MHz, CDCl₃): δ (ppm) 1.18 (12 H, t, J = 6.8 Hz), 3.36 (8 H, q, J = 7.2 Hz), 6.32 (2 H, dd, J₁ = 2.8 Hz, J₂ = 8.8 Hz), 6.44–6.49 (4 H, m), 7.11–7.13 (1 H, m), 7.44–7.49 (2 H, m), 7.93–7.98 (1 H, m)).

indicated that TiO₂ nanoparticles retain their original surface morphology after modification with fluorophore unit (Rh1) (Fig. 6(C)).

3.2. Effect of pH on the Fluorescence Response of the Sensing Material (Rh1@TiO₂)

It was conceived that the fluorophore, Rh1, would respond to acidic pH by going to its ring-opened form. The response of Rh1 at different pH was carried out in CH₃CN–H₂O and the fluorescence response was noted. As the sensing material can be dispersed in water only, the pH dependency study of the sensing material (Rh1@TiO₂) was carried out in water and buffer solutions, and pH was maintained by the addition of acid or base. In the present study, the chosen pH range was 3.0–10.0. The fluorimetric response was negligible at the neutral and basic pH, but surge up in the acidic pH. The highest response was seen at pH 5 (Fig. 7).

The response of Rh1@TiO₂ towards orthosilicic acid was also measured at the same pH range. Strongly alkaline pH was avoided as basic metal silicates precipitate out at this condition.^{65,66} The strong acidic condition was also avoided as cells cannot bear such harsh condition. Figure 8 shows the fluorescence responses of Rh1@TiO₂

as a function of pH in the presence and absence of orthosilicic acid. As expected, Rh1@TiO₂ started emitting strong fluorescence signals as the pH of the solution went below 7. The fluorescence output showed steady rise up to pH 3 (excited at 525 nm). This was well-expected, considering the possibility of protonation of the spiro lactam ring of Rh1 which leads to the formation of the fluorescent ring-open state in Rh1 under acidic pH. However, the sensing material, Rh1@TiO₂ showed very weakly to negligible fluorescence response at pH ≥ 7, suggesting that the spirocyclic form of the probe molecule remained intact at this pH condition. The pH-controlled emission measurements established that Rh1 and Rh1@TiO₂ could be applied for the detection of the incessant release of H⁺ from a hydrated form of silica (viz. orthosilicic acid). Considering the fact that the detection of silica species bioaccumulation *in-vitro* or *in-vivo* would require cellular pH, the media for fluorometric detection of orthosilicic acid was set at pH 7.0 for further studies.

3.3. Spectrofluorometric and Spectrophotometric Titrations of Orthosilicic Acid by Rh1@TiO₂

To comprehend the toxic silica species (viz. orthosilicic acid) sensing abilities of Rh1@TiO₂, fluorescence

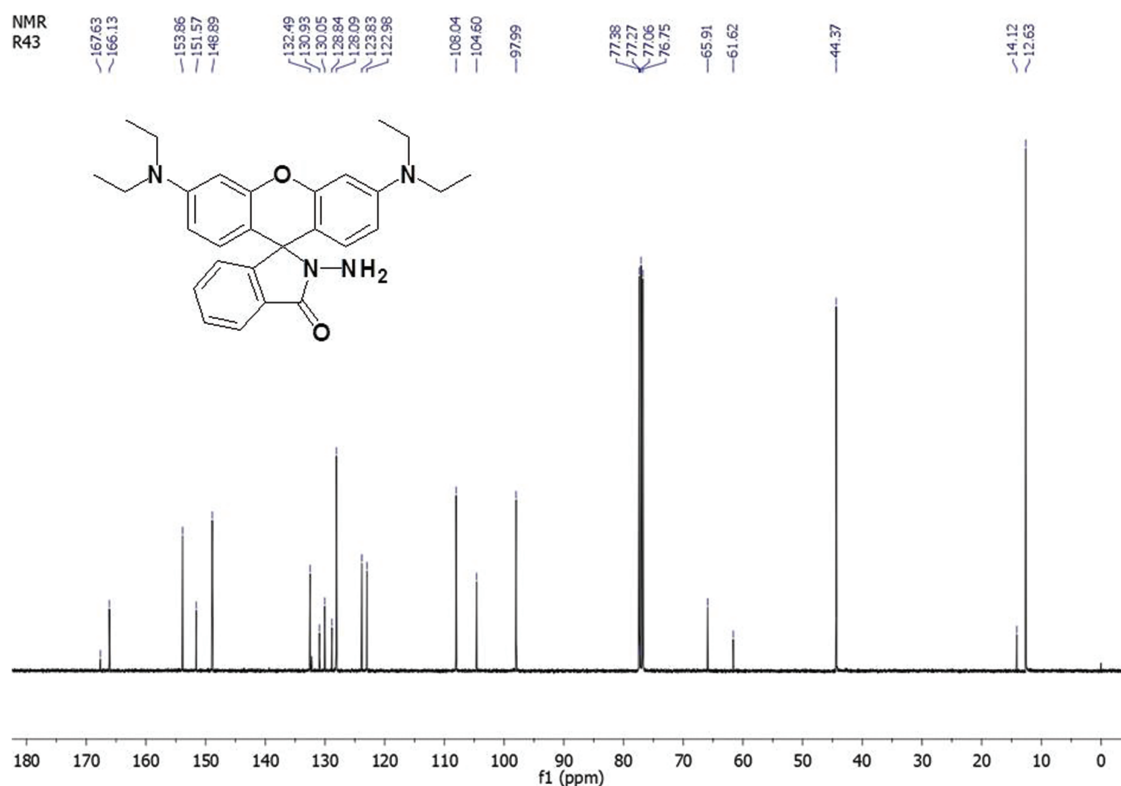


Figure 2. ¹³C NMR spectra of Rh1 (¹³C NMR (CDCl₃, 100 MHz): δ (ppm) 12.62, 44.37, 65.91, 97.98, 104.62, 108.03, 122.27, 123.83, 128.08, 128.84, 130.05, 130.93, 132.49, 148.88, 151.56, 153.85, 166.13).

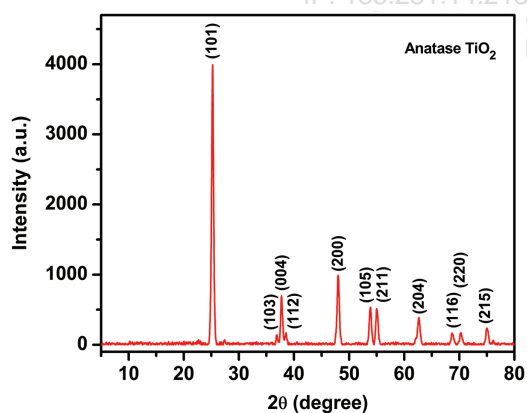


Figure 3. XRD spectra of the synthesized TiO₂ nanoparticles.

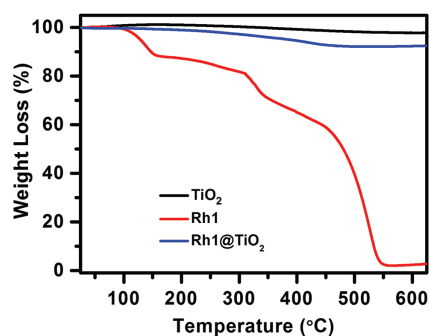


Figure 4. TGA curves of TiO₂ nanoparticles (black line), probe Rh1 (red line) and sensing material Rh1@TiO₂ (blue line).

response of an aqueous dispersion of the sensing material upon steady addition of 0–100 μL of 10 mM (0.0–33.3 mg/L) of orthosilicic acid was measured. The fluorescence output of fluorophore unit (Rh1) at λ_{max} = 585 nm was intensified with the incremental addition of orthosilicic acid, up to 12 fold, demonstrating quick recognition efficacy (Fig. 9). This is the outcome of the transformation of the non-fluorescent spirolactam form of Rh1 in the sensing material to its ring-opened fluorescent state on reacting with H⁺ ions released by orthosilicic acid. Additionally, a separate time-dependent fluorescence

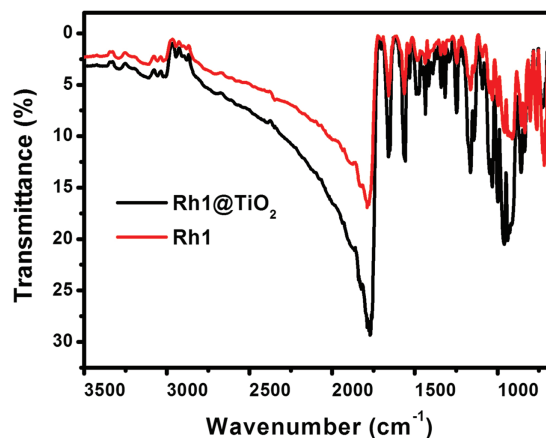


Figure 5. IR spectra of Rh1 and the sensing material, Rh1@TiO₂.

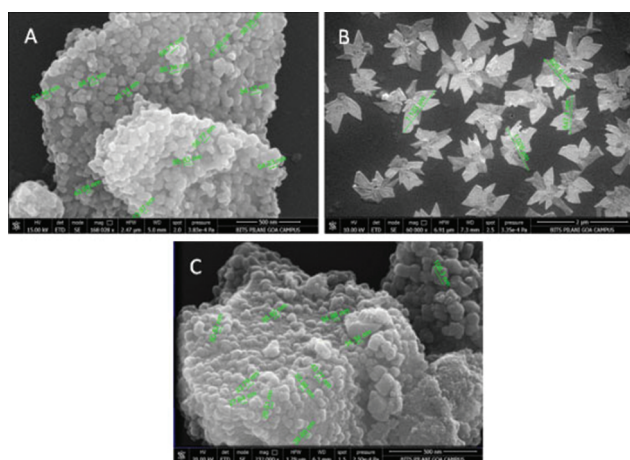


Figure 6. FESEM images of (A) anatase TiO₂ nanoparticles; (B) free Rh1 and (C) the sensing material, Rh1@TiO₂.

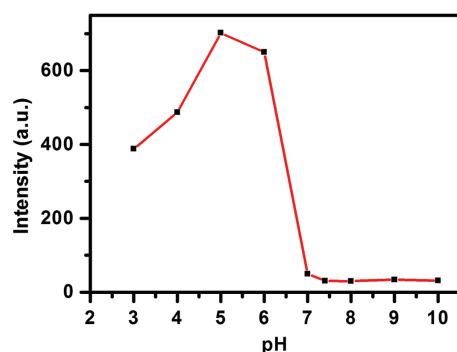


Figure 7. The effect of pH on the fluorescence response of Rh1 probe at different pH in 20% CH₃CN–H₂O.

measurement of an equimolar mixture of Rh1@TiO₂ and orthosilicic acid (both 10 mg/L) revealed that 10 min of incubation is sufficient in obtaining the highest fluorescence response suggesting a quick conversion to the spiro-lactam form approach in the presence of H⁺ ions.

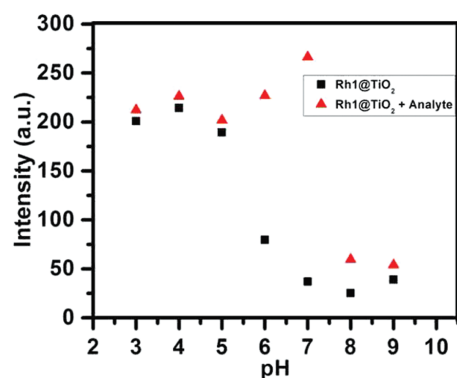


Figure 8. The fluorescence response of Rh1@TiO₂ sensing system (10 mg/L) after 10 min with and without orthosilicic acid (10 mg/L, 1:1 ratio) in different pH buffers (pH 3.0–10.0) at room temperature (λ_{ex} = 525 nm).

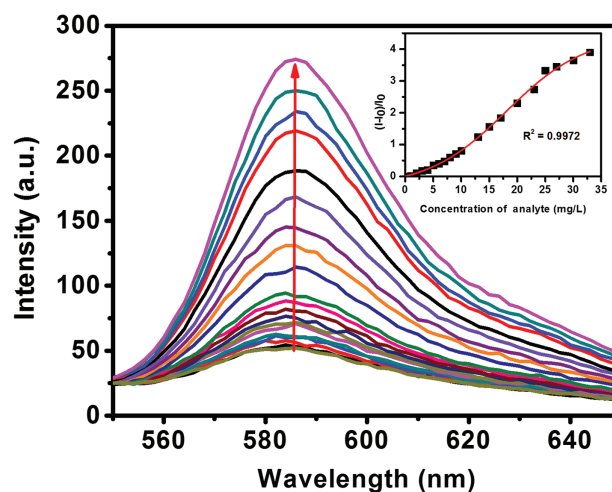


Figure 9. Fluorescence response of Rh1@TiO₂ sensing system (10 mg/L) upon addition of orthosilicic acid (0.0–33.3 mg/L) in deionized water at room temperature after 10 min [excitation at λ_{max} = 525 nm]. Inset: Plot of the increment in emission against the concentration of the analyte.

In a similar study, the chromogenic response of the Rh1@TiO₂ towards orthosilicic acid was investigated by the absorbance measurements of an aqueous probe solution on steady addition of 0–100 μ L of 10 mM solution of orthosilicic acid (or 0.0–33.3 mg/L). The absorbance signal peak, at λ_{max} = 558 nm, was found to be intensified with increasing orthosilicic acid doses in solution (Fig. 10). Both the investigations strongly portrayed the efficacy of the probe in H⁺ ion detection (from orthosilicic acid) in aqueous solutions.

3.4. Mechanistic Aspects of Silica Species Sensing by Rh1@TiO₂ and Spectral Features

The spiro-lactam form of rhodamine derivatives (viz. Rh1 and sensing material, Rh1@TiO₂) is non-fluorescent and colourless at neutral pH. However, binding with H⁺ ions (from orthosilicic acid) induces a strong orange fluorescence peak and an intense pink colour due to spontaneous conversion of the spiro-lactam form of rhodamine residue

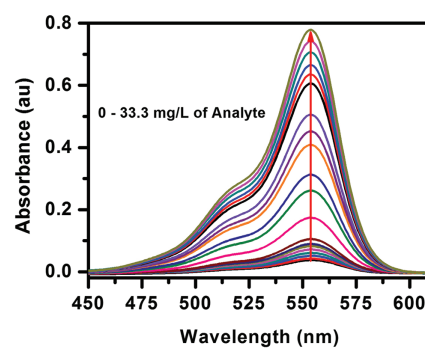
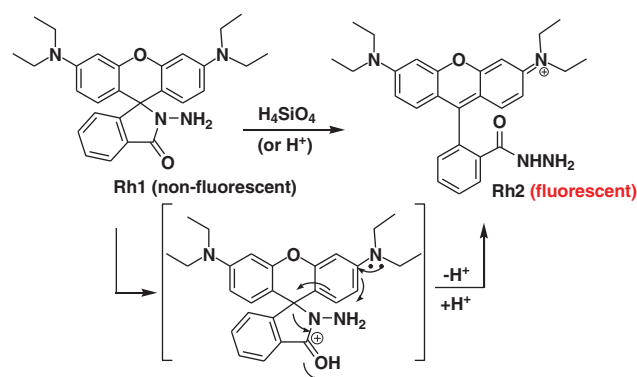


Figure 10. Absorbance response of the Rh1@TiO₂ sensing system (10 mg/L) after 10 mins of the addition of orthosilicic acid (0.0–33.3 mg/L) in deionized water at room temperature.



Scheme 2. A plausible mechanism of the H⁺ mediated ring opening of Rh1 in the process of detecting orthosilicic acid.

to its ring-opened form, Rh2 (Scheme 2).^{23,59} This phenomenon is justified by the appearance of an anticipated peak of the ring-opened form of rhodamine B hydrazide at 586 nm in the emission spectra. The formation of the ring-opened form (Rh2) was confirmed by carrying out a reaction of Rh1 in the presence of orthosilicic acid at a larger scale and taking IR and NMR of the isolated product and matching with reported data.⁵⁹

3.5. Fluorescence Response at Different Time Intervals

The probe Rh1 was previously reported by Czarnik⁵² for Cu²⁺ and Chang⁵⁸ for Hg²⁺ detection. However, we observed that the sensing material (Rh1@TiO₂) hardly shows any fluorimetric response in the presence of Cu²⁺ and Hg²⁺ ions under the sensing condition for orthosilicic acid (Figs. 11–14). These observations insisted us to carry out a time-dependent study for both Cu²⁺ and Hg²⁺ ions in water. In a separate study, we have repeated the studies of Czarnik⁵² and Chang.⁵⁸ In the present study, free probe, i.e., Rh1, was separately treated with Cu²⁺, Hg²⁺, Fe³⁺, Zn²⁺ and H₄SiO₄ in 20% CH₃CN-HEPES buffer (at pH 7) and 10% CH₃OH-phosphate buffer (at pH 7) and the fluorescence response was noted after 30 min, 2 h, and 6 h. It was observed that Rh1 is a very effective sensor for Cu²⁺ in 20% CH₃CN-HEPES buffer with the highest response after 30 min (Fig. 11(A)). However, Hg²⁺ started

to show a response after 2 h and surpasses Cu²⁺ after 6 h (Figs. 11(B and C)). In 10% CH₃OH-phosphate buffer Hg²⁺ showed a strong response, whereas other metal ions showed a negligible response (Fig. 12). In both the cases, H₄SiO₄ did not show any response as the availability of H⁺ was restricted by buffer medium.

In a separate study, the sensing material, Rh1@TiO₂ was separately treated with Cu²⁺, Hg²⁺, and H₄SiO₄ in water and the fluorescence response was noted after 10 min, 30 min, and 6 h (Fig. 13). While H₄SiO₄ started to show strong response immediately after 10 min, the fluorimetric response of Hg²⁺ picked up only after 6 h of exposure (Fig. 13(C)). Presumably, the approach of Hg²⁺ ions was somewhat restricted inside the core of the sensing material (Rh1@TiO₂) and therefore, the chemodosimeter (Rh1) does not get quick access to these cations to react with. This resulted in a very low fluorometric response in water after 10 min.

3.6. Selectivity Study with Interfering Metal Ions

Kidneys, specifically the proximal tubular cells are actively involved in maintaining a balance of major elements in the body viz. Na⁺, K⁺, Mg²⁺ and trace elements, like Fe²⁺, Fe³⁺, Mn²⁺, Zn²⁺ ions, and thereby inherently contain these cationic species which are essential for various cellular functions, such as heart and muscle contractions, nerve signalling, hormone production, anti-oxidative enzyme action, haemoglobin formation, glucose homeostasis, and renoprotective effects.^{69,70} These organs additionally serve as the primary target of metal toxicity owing to its high reabsorptive and accumulative properties. Some of the metal species are well-reported to inflict severe nephrotoxicity when surpassing the permissible levels of Ca²⁺, Cd²⁺, Co²⁺, Hg²⁺, Pb²⁺, Sr³⁺.^{71,72} The specificity of Rh1@TiO₂ sensing material for a toxic hydrated form of silica (viz. orthosilicic acid) in an aqueous solution was examined analogously in the presence of various competing toxic and inherent renal metal ions under comparable conditions. For this purpose, the fluorescence responses of Rh1@TiO₂ after addition of equal mixture (10 mg/L) of each metal ion (Ca²⁺, Cd²⁺, Co²⁺, Cu²⁺, Fe²⁺, Fe³⁺, Hg²⁺, Na⁺, K⁺, Mg²⁺, Mn²⁺, Pb²⁺, Sr³⁺, Zn²⁺) and orthosilicic

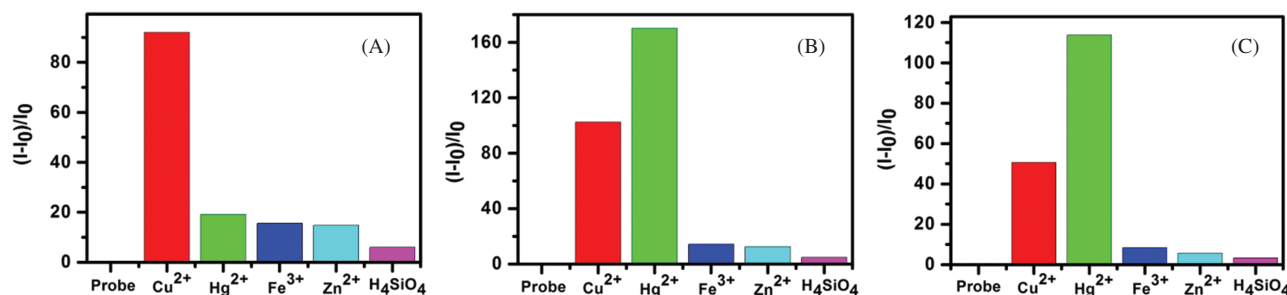


Figure 11. Time-dependent study of Cu²⁺, Hg²⁺, H₄SiO₄ and other metal ions against Rh1 after (A) 30 min, (B) 2 h and (C) 6 h in 20% CH₃CN-HEPES buffer (at pH 7).

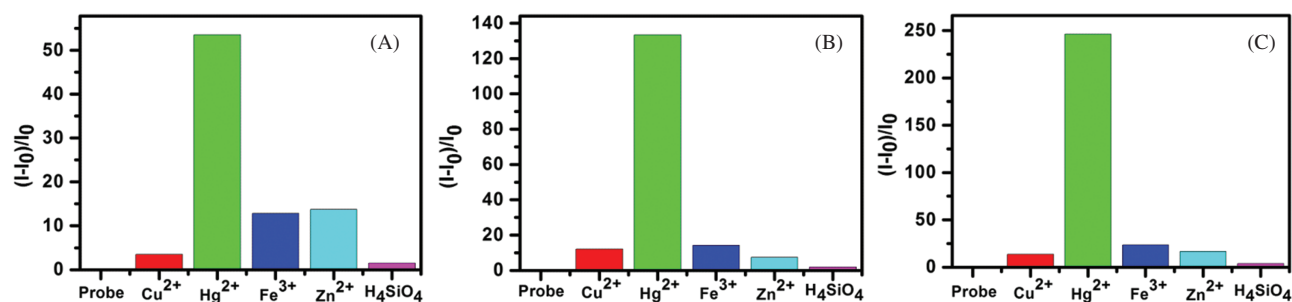


Figure 12. Time-dependent study of Cu²⁺, Hg²⁺, H₄SiO₄ and other metal ions against Rh1 after (A) 30 min, (B) 2 h and (C) 6 h in 10% CH₃OH-Phosphate buffer (at pH 7).

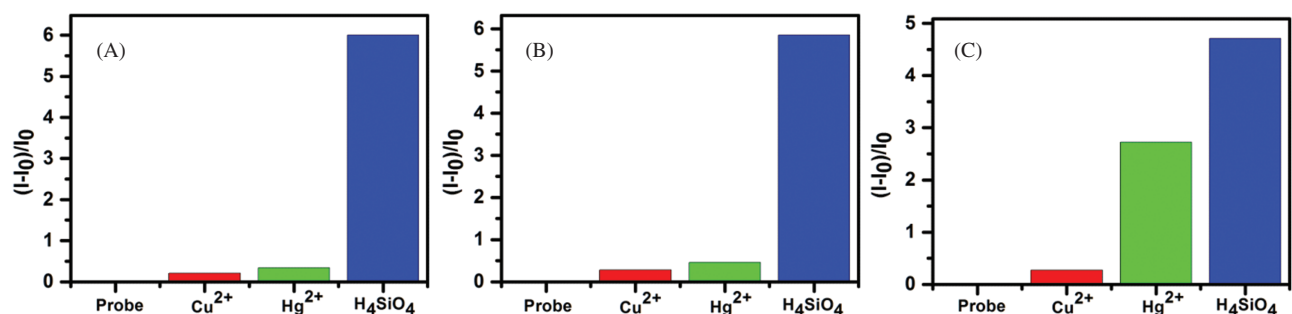


Figure 13. Time-dependent study of Cu²⁺, Hg²⁺ and H₄SiO₄ and other metal ions against Rh1@TiO₂ after (A) 10 min, (B) 30 min, (C) 6 h in water.

acid (H₄SiO₄ which acts as a source of H⁺) in the aqueous dispersion of sensing material (10 mg/L) were recorded (Fig. 14).

As represented in Figure 14, the sensing material, Rh1@TiO₂ exhibited negligible to no response for most of the potential rival metal ions and generated a strong fluorescence response upon interaction with orthosilicic acid at the working pH. Notably, low response aroused out of interaction with Hg²⁺, Zn²⁺, Fe²⁺ or Co²⁺ under the sensing condition. This is in sheer contrast with the reported results by Czarnik⁵² for Cu²⁺ and Chang⁵⁸ for Hg²⁺ with Rh1. We repeated their studies

and got similar results as per their reports for Rh1 when it is free. However, in a separate study, it was observed that Rh1@TiO₂ responds to Hg²⁺ after long exposure in water (Fig. 13). Presumably, the approach of larger metal ions is somewhat restricted inside the core of the sensing material (Rh1@TiO₂) and therefore, the chemodosimeter (Rh1) does not get quick access to these cations to react with. This results in very low fluorometric response at pH 7 after 10 min. The fluorescence output in the presence of these cations is still very nominal under the sensing condition making the probe practically unperturbed by the presence of the interfering metal ions. This fact is further established through competition experiments conducted in the presence of large excess (5 times of orthosilicic acid)

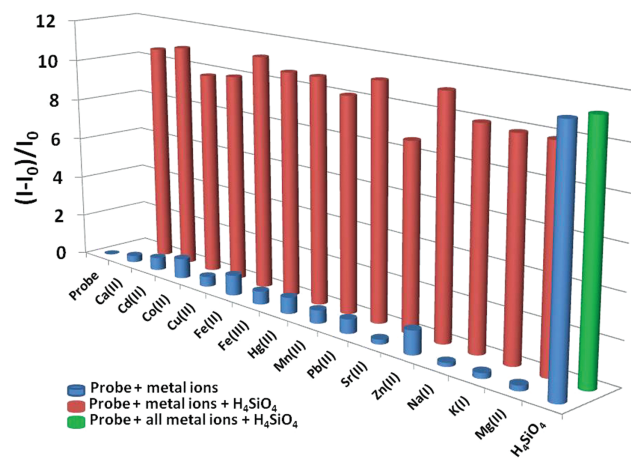


Figure 14. Maximum fluorescence responses of Rh1@TiO₂ (10 mg/L), which were recorded after 10 min of the addition of equal amount of various analytes (metal ions), in deionized water at room temperature.

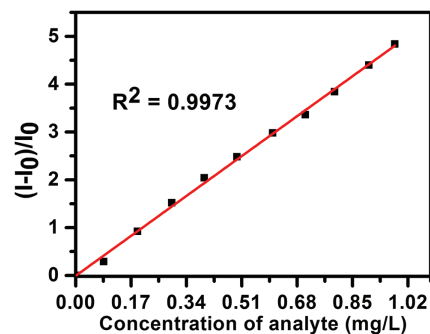


Figure 15. A plot of relative fluorescence intensity versus concentration of analyte obtained from a solution of sensing material Rh1@TiO₂ (10 mg/L) and lower concentration range of orthosilicic acid (0.1–1 mg/L) after 10 min of interaction.

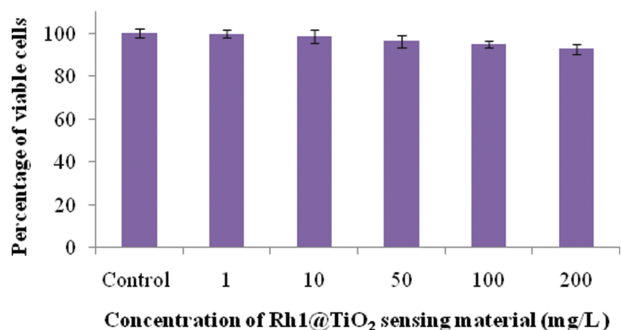


Figure 16. Cytotoxicity study of the sensing material, Rh1@TiO₂ on HK cells at varying doses for 24 h.

of all metal ions and orthosilicic acid (Fig. 14). As anticipated, the orthosilicic acid induced fluorescence response of the sensing material, Rh1@TiO₂ was unaltered by the existence of the competing metal ions, suggesting that the presence of H⁺ ions amidst several other cations is univocally identified by the sensing material with no loss in fluorescence output. The response of the sensing material towards orthosilicic acid amongst diverse nephrotoxic and inherent renal metallic species in an aqueous solution extends its application for selective *in-vitro* detection of toxic silica species accumulation in affected kidney cells or elsewhere.

3.7. Determination of the Detection Limit

The limit of detection (LOD) is an essential property of a sensing system, assessed to gauge its utility for real sample analysis. To elucidate the LOD, the fluorescence output of Rh1@TiO₂ at lower concentrations of orthosilicic acid in deionised water was plotted (Fig. 15). Under prevailing conditions, the sensing material, Rh1@TiO₂ responds linearly to the varying concentration of orthosilicic acid (0.1–1 mg/L or 0.3–3.0 μL in 3 mL) with R² = 0.9973 and

from this, the detection limit was calculated to be 8.4 ppb or 8.4 × 10⁻⁸ M of orthosilicic acid.

3.8. Determination of Cytotoxicity of Rh1@TiO₂ and Fluorescence Imaging of Toxic Silica Species in Live Cells

If a sensing system is intended to apply to live biological species, it is essential to check its biocompatibility and cytotoxicity. As a model human kidney cell system viz. HK cells (Human Kidney cells) was chosen for cytotoxicity study and detection of the toxic silica sp. (specifically orthosilicic acid) accumulation via cellular imaging. Accordingly, the cytotoxicity of different concentrations of Rh1@TiO₂ to HK cells was assessed using MTT assay to determine cell sustainability at an ideal probe concentration. For this, 70% confluent HK cells were exposed to enhancing Rh1@TiO₂ sensing system concentrations, serially diluted in DMEM (i.e., 1, 10, 50, 100, and 200 mg/L) in a 24 well plate, and incubated for 24 h. Unexposed control was simultaneously maintained. The percentages of viable cells relative to untreated controls were determined and plotted (Fig. 16). The cell viability was ascertained to be greater than 90% on 24 h exposure to the highest Rh1@TiO₂ concentration (200 mg/L). This suggests that even high Rh1@TiO₂ concentrations are non-toxic to the living human cells and can be employed for detection of toxic silica species viz. orthosilicic acid bioaccumulation in living organisms.

Since no cytotoxic effect of Rh1@TiO₂ was detected, a median concentration of Rh1@TiO₂ (i.e., 50 mg/L) was employed for fluorescence monitoring of orthosilicic acid deposition in HK cells, which were exposed to increasing doses of orthosilicic acid. The orthosilicic acid deposition over the 1st time point was monitored by pre-treating four sets of HK cells with increasing doses of orthosilicic acid (0.1 mg/L (Fig. 17), 1 mg/L, 10 mg/L and 100 mg/L)

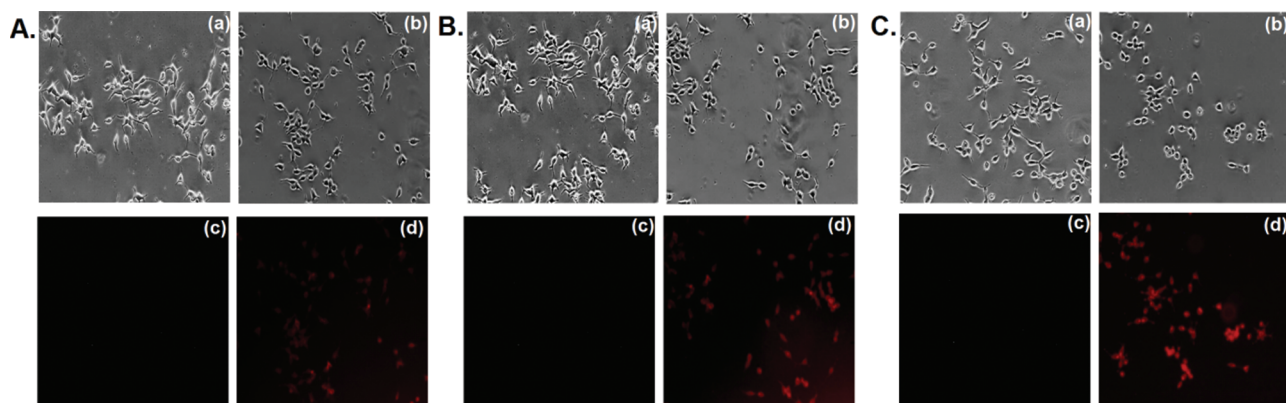


Figure 17. Time-dependent fluorescence detection of toxic silica species (specifically orthosilicic acid) deposition in HK cells treated with low orthosilicic acid (0.1 mg/L) utilizing sensing material, Rh1@TiO₂. HK cells incubated with 0.1 mg/L orthosilicic acid for three different exposure periods viz. 30 min (A), 24 h (B) and 8 days (C) followed by treatment with 50 mg/L of Rh1@TiO₂ sensing material (for 30 min) after each dosing period. Images recorded after sensing material exposure in the absence (a, c) and presence (b, d) of orthosilicic acid at each temporal point. Scale bars are 200 μm.

for 1 h, followed by PBS washing to remove the non-accumulated species. This was followed by incubation with 50 mg/L of the Rh1@TiO₂ for 30 min at 37 °C and 5% CO₂ succeeded by a triple PBS wash (to remove excess

sensing-system) and fluorescence images were captured (Fig. 18). These steps were replicated for the separate sets of cells pre-incubated with orthosilicic acid for 24 h and 8 days, respectively. At each time point, set of HK

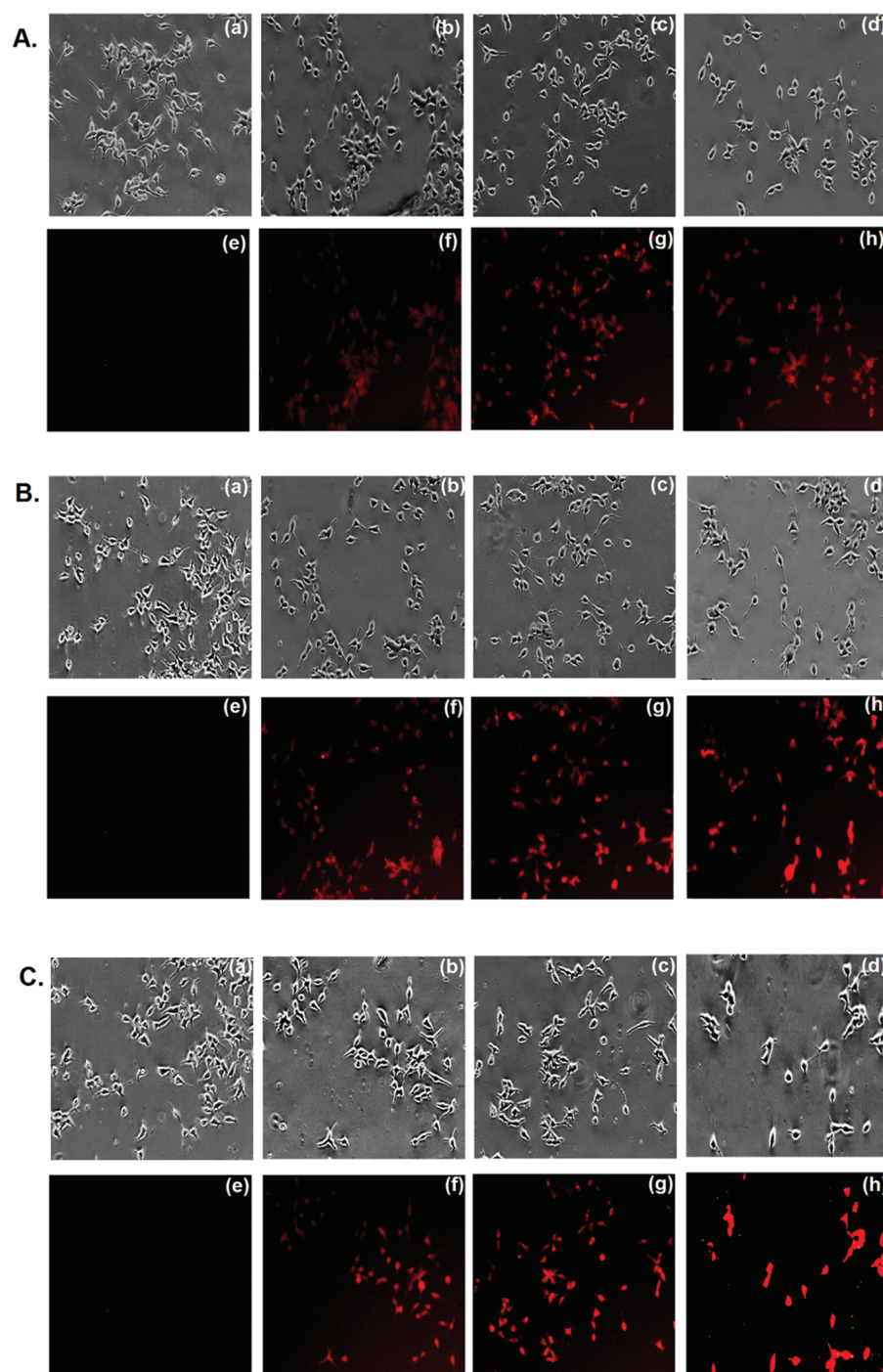


Figure 18. Dose and time-dependent monitoring of toxic silica species (viz. orthosilicic acid) accumulation in live HK cells with the sensing material, Rh1@TiO₂. Phase contrast (b–d) and fluorescence images (f–h) of HK cells on treatment with 1 mg/L (b, f), 10 mg/L (c, g) and 100 mg/L (d, h) of orthosilicic acid for three different exposure time points viz. 1 h (A), 24 h (B) and 8 days (C) followed by 30 min incubation with Rh1@TiO₂ (50 mg/L) at each temporal point. Images of HK cells (a, e) were captured at each time point in the absence of orthosilicic acid and presence of Rh1@TiO₂ to serve as controls. Gradual escalation in fluorescence intensity noted with increasing orthosilicic acid doses and exposure period signifying progressive intracellular accumulation of toxic silica species inflicting chronic nephrotoxicity. Scale bars are 200 μ m.

cells were separately incubated with solely 50 mg/L of Rh1@TiO₂ in the absence of orthosilicic acid for 30 min to serve as probe controls negating the possibility of intrinsic fluorescence of the Rh1@TiO₂ sensing material, justified by the absence of fluorescence as recorded by fluorescence microscope (Fig. 18).

As depicted in Figure 18, significant orange fluorescence was observed from the intracellular region of nephrotoxic HK cells contaminated with orthosilicic acid and consequently treated with the probe Rh1@TiO₂. It can be considered that the nanosize of the probe helps to smoothly cross the cell membrane and subsequent interact with the accumulated silica (in the form of orthosilicic acid) to get converted to its ring-opened fluorescent form of Rh1. The fluorescence intensity was apparently a function of the dose and time of orthosilicic acid exposure manifested by an enhanced response on exposure to the highest orthosilicic acid dose (100 mg/L) for the longest period (8 days) due to more and more interaction with intercellular H⁺ ions leading to fluorescent ring-opened state of the probe. However, the cell density diminishes on exposure to higher doses of silica species (orthosilicic acid) over a longer period of time highlighting dose and time-dependent toxicity. Notably, the sensitivity of this analytical tool was found to be very high as the accumulation of low concentration orthosilicic acid (0.1 mg/L) in HK cells is good enough to generate sufficiently strong fluorescence signals from the intra-cellular region (Fig. 17). This study provides substantial evidence on the ability of this sensing material to detect silica species accumulation in human kidney cells on chronic exposure to increasing dosages that inflicts severe nephrotoxicity ultimately manifesting as Chronic Kidney Disease. A low-level detection and imaging of silica in affected HK cells may lead to the conclusion that the sensing material, Rh1@TiO₂ can eventually be employed for *in-vitro* monitoring of toxic silica species bioaccumulation in any biological samples.

4. CONCLUSIONS

In summary, the present work demonstrates an effective strategy to detect and image the toxic silica species (orthosilicic acid) accumulation in the live cells. The sensing material Rh1@TiO₂ was prepared by simple physisorption of a rhodamine derivative, which acts as a chemodosimeter based pH sensor, onto the biocompatible, non-toxic TiO₂ nanoparticles. This newly developed water-dispersible fluorescent nanoprobe has demonstrated its capability to detect orthosilicic acid in aqueous media, and in biological systems via interaction with the incessantly released H⁺ ions. The H⁺ ions generate the fluorescent ring-opened form of the fluorophore and result in a strong orange fluorescence output.

The studies were carried out on human kidney cells at biological pH (pH 7). The cell imaging studies confirmed that this probe is biocompatible and can easily

cross the cellular surface of nephrotoxic HK cells interacting with bioaccumulated orthosilicic acid produced under silica stress conditions. The synthesized sensing material Rh1@TiO₂ offers several advantages like good water dispersibility, the absence of organic solvents during fluorimetric studies, quick turn-on type signal transduction, low-level imaging. This sensing material has the potential to be used in the medical tool for early identification of silica-induced nephrotoxicity with effective detection and imaging of toxic silica species deposition in the exposed kidney cells intending to adopt necessary prophylactic measures to reduce the burden and risk of chronic kidney disease development.

Abbreviations

CKD—Chronic Kidney Disease; DMEM—Dulbecco's Modified Eagle's Medium; HK—human kidney cells; H₄SiO₄—orthosilicic acid; MTT—3-(4,5-Dimethylthiazol-2-yl)-2,5-Diphenyltetrazolium Bromide; PBS—Phosphate buffered saline; P-XRF—portable X-ray fluorescence spectrometer; RA—Rheumatoid arthritis; Rh1—Rhodamine B hydrazide; Rh1@TiO₂—Rhodamine hydrazide adsorbed onto TiO₂ nanoparticles; SiO₂—Silica; SLE—systemic lupus erythematosus; TiO₂—titanium dioxide.

Declaration of Interest

The authors declare no personal, financial or organisational conflict of interests.

Acknowledgments: Amrita Chatterjee thanks UGC-DAE (CSR-KN/CRS-91/2016-17/1132) and DST-SERB (project No. EMR/2016/001416) for financial support. Starlaine C. Mascarenhas and Ram U. Gawas are grateful to BITS, Pilani for research fellowships. The authors are thankful to the central NMR Facility of BITS Pilani, Pilani campus for NMR spectral data and Central Sophisticated Instrumentation Facility (CSIF) of BITS Pilani KK Birla Goa Campus for LC-MS data and FESEM images.

References and Notes

1. J. Marin-Carbonne, F. Robert, and M. Chaussidon, *Precambrian Res.* 247, 223 (2014).
2. J. T. Cornelis and B. Delvaux, *Funct. Ecol.* 30, 1298 (2016).
3. M. M. Mendez-Vargas, F. B. Baez-Revueltas, P. Lopez-Rojas, J. HoracioTovalin-Ahumada, J. O. Zamudio-Lara, I. A. Marin-Cotoñieto, and F. Villedaf, *Rev. Med. Inst. Mex. Seguro. Soc.* 51, 384 (2013).
4. K. M. Bang, J. M. Mazurek, J. M. Wood, G. E. White, and S. A. Hendricks, *Morb. Mortal. Wkly. Rep.* 64, 117 (2015).
5. K. Tsuchiya, M. Toyoshima, Y. Kamiya, Y. Nakamura, S. Baba, and T. Suda, *Internal Med.* 56, 1701 (2017).
6. V. Malmstrom, A. I. Catrina, and L. Klareskog, *Nat. Rev. Immunol.* 17, 60 (2017).
7. S. Lee, H. Matsuzaki, N. Kumagai-Takei, K. Yoshitome, M. Maeda, Y. Chen, and Y. Nishimura, *Environ. Health. Prev.* 19, 322 (2014).

8. I. Marie, J. F. Gehanno, M. Bubenheim, A. B. Duval-Modeste, P. Joly, S. Dominique, P. Bravard, D. Noel, A. F. Cailleux, J. Weber, and P. Lagoutte, *Autoimmun. Rev.* 13, 151 (2014).
9. K. Steenland and E. Ward, *Cancer. J. Clin.* 64, 63 (2014).
10. S. Sen, R. Mitra, S. Mukherjee, P. K. Das, and S. Moitra, *Curr. Respir. Med. Rev.* 12, 56 (2016).
11. N. Ghahramani, *Int. J. Occup. Environ. Med.* 1, 108 (2010).
12. M. L. Millerick-May, S. Schrauben, M. J. Reilly, and K. D. Rosenman, *Am. J. Ind. Med.* 58, 730 (2015).
13. M. Ricco, E. Thai, and S. Cella, *Ind. Health* 54, 74 (2016).
14. T. Nishizono, S. I. Eta, H. Enokida, K. Nishiyama, M. Kawahara, and M. Nakagawa, *Int. J. Urol.* 11, 119 (2004).
15. S. Mascarenhas, S. Mutnuri, and A. Ganguly, *Chemosphere* 177, 239 (2017).
16. S. Kumar, Y. Milstein, Y. Brami, M. Elbaum, and R. Elbaum, *New Phytol.* 213, 791 (2017).
17. E. McLarnon, S. McQueen-Mason, I. Lenk, and S. E. Hartley, *Front. Plant. Sci.* 8, 1199 (2017).
18. B. Tesson and M. Hildebrand, *Plos One* 5, e14300 (2010).
19. T. Ueno and T. Nagano, *Nat. Methods* 8, 642 (2011).
20. T. Terai and T. Nagano, *Pflug. Arch. Eur. J. Phy.* 465, 347 (2013).
21. M. Beija, C. A. Afonso, and J. M. Martinho, *Chem. Soc. Rev.* 38, 2410 (2009).
22. J. Chan, S. C. Dodani, and C. J. Chang, *Nat. Chem.* 4, 973 (2012).
23. H. N. Kim, M. H. Lee, H. J. Kim, J. S. Kim, and J. Yoon, *Chem. Soc. Rev.* 37, 1465 (2008).
24. Q. A. Best, R. Xu, M. E. McCarroll, L. Wang, and D. J. Dyer, *Org. Lett.* 12, 3219 (2010).
25. M. Tian, X. Peng, J. Fan, J. Wang, and S. Sun, *Dyes Pigments* 95, 112 (2012).
26. L. Liu, P. Guo, L. Chai, Q. Shi, B. Xu, J. Yuan, and W. Zhang, *Sensor. Actuat. B-Chem.* 194, 498 (2014).
27. M. A. Brzezinski and D. J. Conley, *J. Phycol.* 30, 45 (1994).
28. M. Kucki and T. Fuhrmann-Lieker, *J. R. Soc. Interface* 9, 727 (2012).
29. S. Su, W. Wu, J. Gao, J. Lu, and C. Fan, *J. Mater. Chem.* 22, 18101 (2012).
30. C. E. Rowland, C. W. Brown, J. B. Delehanty, and I. L. Medintz, *Mater. Today* 19, 464 (2016).
31. P. Kumar, K. H. Kim, V. Bansal, S. Kumar, N. Dilbaghi, and Y. H. Kim, *Trend. Anal. Chem.* 86, 235 (2017).
32. L. Walekar, T. Dutta, P. Kumar, Y. S. Ok, S. Pawar, A. Deep, and K. H. Kim, *Trend. Anal. Chem.* 97, 458 (2017).
33. J. Yao, M. Yang, and Y. Duan, *Chem. Rev.* 114, 6130 (2014).
34. Q. Liu, Q. Zhou, and G. Jiang, *Trend. Anal. Chem.* 58, 10 (2014).
35. J. Schneider, M. Matsuoka, M. Takeuchi, J. Zhang, Y. Horiuchi, M. Anpo, and D. W. Bahnemann, *Chem. Rev.* 114, 9919 (2014).
36. H. Chen, C. E. Nanayakkara, and V. H. Grassian, *Chem. Rev.* 112, 5919 (2012).
37. T. Rajh, N. M. Dimitrijevic, M. Bissonnette, T. Koritarov, and V. Konda, *Chem. Rev.* 114, 10177 (2014).
38. A. A. Keller, H. Wang, D. Zhou, H. S. Lenihan, G. Cherr, B. J. Cardinale, and Z. Ji, *Environ. Sci. Technol.* 44, 1962 (2010).
39. Z. Ji, X. Jin, S. George, T. Xia, H. Meng, X. Wang, and A. E. Nel, *Environ. Sci. Technol.* 44, 7309 (2010).
40. C. Zhao, F. U. Rehman, Y. Yang, X. Li, D. Zhang, H. Jiang, and C. Liu, *Sci. Rep.* 5, 11518 (2015).
41. J. S. Taurozzi, V. A. Hackley, and M. R. Wiesner, *Nanotoxicology* 7, 389 (2013).
42. Y. Zhao and H. S. Nalwa (eds.), *Nanotoxicology: Interactions of Nanomaterials with Biological Systems*, American Scientific Publishers, Los Angeles (2007).
43. S. Singh and H. S. Nalwa, *J. Nanosci. Nanotechnol.* 7, 3048 (2007).
44. V. Kumar, M. Banerjee, and A. Chatterjee, *Talanta* 99, 610 (2012).
45. D. G. Khandare, V. Kumar, A. Chattopadhyay, M. Banerjee, and A. Chatterjee, *RSC Adv.* 3, 16981 (2013).
46. D. G. Khandare, H. Joshi, M. Banerjee, M. S. Majik, and A. Chatterjee, *RSC Adv.* 4, 47076 (2014).
47. S. Hazra, S. Balaji, M. Banerjee, A. Ganguly, N. N. Ghosh, and A. Chatterjee, *Anal. Methods* 6, 3784 (2014).
48. D. G. Khandare, H. Joshi, M. Banerjee, M. S. Majik, and A. Chatterjee, *Anal. Chem.* 87, 10871 (2015).
49. A. Chatterjee, D. G. Khandare, P. Saini, A. Chattopadhyay, M. S. Majik, and M. Banerjee, *RSC Adv.* 5, 31479 (2015).
50. D. G. Khandare, M. Banerjee, R. Gupta, N. Kumar, A. Ganguly, D. Singh, and A. Chatterjee, *RSC Adv.* 6, 52790 (2016).
51. A. Chatterjee, M. Banerjee, D. G. Khandare, R. Gawas, S. C. Mascarenhas, A. Ganguly, R. Gupta, and H. Joshi, *Anal. Chem.* 89, 12698 (2017).
52. V. Dujols, F. Ford, and A. W. Czarnik, *J. Am. Chem. Soc.* 119, 7386 (1997).
53. X.-F. Yang, X.-Q. Guo, and Y.-B. Zhao, *Talanta* 57, 883 (2002).
54. X.-F. Yang, X.-Q. Guo, and Y.-B. Zhao, *Anal. Chim. Acta* 456, 121 (2002).
55. Y. Xiang, L. Mei, N. Li, and A. Tong, *Anal. Chim. Acta* 581, 132 (2007).
56. X. Chen, and J. Zou, *Microchim. Acta* 157, 133 (2007).
57. Z. Zhang, Y. Zheng, W. Hang, X. Yan, and Y. Zhao, *Talanta* 85, 779 (2011).
58. K. N. Kim, M. G. Choi, J. H. Noh, S. Ahn, and S.-K. Chang, *Bull. Korean Chem. Soc.* 29, 571 (2008).
59. M. Pandurangappa and S. K. Kumar, *Anal. Methods* 3, 715 (2011).
60. M. Asano, M. Doi, K. Baba, M. Taniguchi, M. Shibano, S. Tanaka, M. Sakaguchi, M. Takaoka, M. Hirata, R. Yanagihara, R. Nakahara, Y. Hayashi, T. Yamaguchi, H. Matsumura, and Y. Fujita, *J. Biosci. Bioeng.* 114, 98 (2014).
61. M. Kang, D. Peng, Y. Zhang, Y. Yang, L. He, F. Yan, S. Sun, S. Fang, P. Wang, and Z. Zhang, *New J. Chem.* 39, 3137 (2015).
62. P. Praikaew, T. Duangdeetip, N. Chimpalee, C. Wainiphithapong, P. Swanglap, and N. Wanichacheva, *Mater. Express* 5, 300 (2015).
63. L. Wang, B. Zheng, Y. Zhao, J. Du, and D. Xiao, *Anal. Methods* 4, 2369 (2012).
64. B. Naik, C. H. Manoratne, A. Chandrashekhar, A. Iyer, V. S. Prasad, and N. N. Ghosh, *J. Exp. Nanosci.* 8, 462 (2013).
65. E. R. Spada, E. A. Pereira, M. A. Montanhera, L. H. Morais, R. G. Freitas, R. G. Costa, and F. R. de Paula, *J. Mater. Sci-Mater. El.* 28, 16932 (2017).
66. A. Adan, Y. Kiraz, and Y. Baran, *Curr. Pharm. Biotechnol.* 17, 1213 (2016).
67. D. Hermosilla, R. Ordonez, L. Blanco, E. de la Fuente, and A. Blanco, *Chem. Eng. Technol.* 35, 1632 (2012).
68. N. A. Milne, T. O'Reilly, P. Sanciole, E. Ostarcevic, M. Beighton, K. Taylor, M. Mullett, A. J. Tarquin, and S. R. Gray, *Water Res.* 65, 107 (2014).
69. U. C. Gupta and S. C. Gupta, *Pedosphere* 24, 13 (2014).
70. A. Agarwal, P. Khanna, D. K. Baidya, and M. K. Arora, *J. Clin. Endocrinol. Metab.* 1, 57 (2011).
71. A. Wilk, E. Kalisińska, D. I. Kosik-Bogacka, M. Romanowski, J. Rozanski, K. Ciechanowski, and N. Lanocha-Arendarczyk, *Environ. Geochem. Hlth.* 39, 889 (2017).
72. S. E. Orr and C. C. Bridges, *Int. J. Mol. Sci.* 18, 1039 (2017).

Received: 10 June 2018. Accepted: 2 July 2018.